Suppression of back-to-back particle–antiparticle correlations in high energy nuclear collisions

Jörn Knoll[1,*]

[1] *GSI Helmholtzzentrum für Schwerionenforschung GmbH, Planckstr. 1, 64291 Darmstadt, Germany*

(Dated: February 27, 2011)

Analytical formulae are presented which provide quantitative estimates for the suppression of the anticipated back-to-back particle–antiparticle correlations in high energy nuclear collisions, both, due to the finite duration of the transition dynamics and due to the continuous freeze-out. They show that it is unlikely to observe the effect.

PACS numbers: 14.40.-n
Keywords: particle–antiparticle correlations, heavy-ion collisions

I. INTRODUCTION

In 1996 Asakawa and Csörgő [1] suggested that back-to-back particle–antiparticle correlations should be observable in high-energy nuclear collisions, see also earlier considerations in Refs. [2, 3]. Based on a sudden transition assumption huge effects were predicted for this phenomenon. In a subsequent paper together with Gyulassy [4] it was shown that the finite duration τ of the transition reduces the effect. In that paper, however, the authors used a discontinuous and therefore unrealistic transition profile that led to large ultraviolet Fourier components and thus to a very moderate reduction of the effect of order $1/((2\omega\tau)^2+1)$. Here 2ω is the energy required to produce the pair. About a further dozen applications based on this unrealistic assumptions followed, cf. e.g. Ref. [5] and earlier references therein.

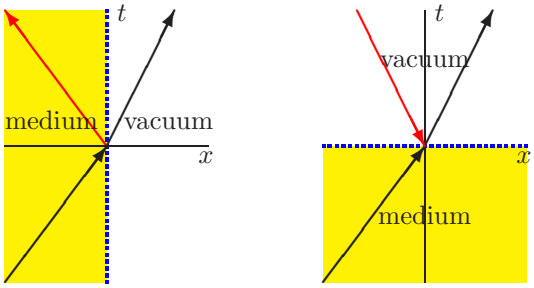

FIG. 1: Optical ray pictures in space-time. Left: the standard reflection-transmission situation, where a wave traverses from one medium (yellow) to another one (e.g. vacuum) at a spatial interface. Right: the sudden transition in time from the medium to the vacuum; here the frequency ω is discontinuous, creating a second component with negative ω which has the interpretation of an antiparticle with opposite momentum. The (blue) dashed line separates the media, the arrow sense distinguishes between particle and antiparticle. By means of Lorentz transformations the concept can directly be generalized to hyper-planes and even to curved hyper-surfaces.

*e-mail:j.knoll@gsi.de

In this note the continuous and smooth transition case will be reinvestigated by analytical means, estimating the pair-creation rate due to the in-medium changes of the particles masses induced by a time dependent mean field and also due to the suppression caused by the freeze-out process. Thereby analytical constraints resulting from the underlying equations of motion play an important role. This leads to a suppression factor, which is at least of exponential form $\sim \mathrm{e}^{-4\omega\tau}$ or even steeper, where τ is corresponding transition duration.

II. THE SUDDEN PICTURE

The main assumption of the original approach [1] is the sudden change from the in-medium situation to that in vacuum. The authors used the Bogolioubov-Valatin (BV) transformation to describe the effect, a picture that may not be so intuitive for many of us. Indeed the effect is nothing else than a standard "reflection–transmission" problem at the interface of two media, a well known problem in physics, in particular in optics. Thus, transcribing our wisdom from the spatial situation, like a wave traversing from one medium to another one at a sharp interface (see Fig. 1 left) to the here considered sudden transition in time (Fig. 1 right), precisely recovers the results presented in [1, 4]. The common boundary condition is, that one has one incoming wave and two time-forward propagating outgoing wave components. As in Refs. [1, 4] we restrict the discussion to (charged) relativistic bosons described by the Klein-Gordon (KG) equation. For the sudden case the wave functions with positive and negative energies prior and post to the sudden transition can then be written as (using units with $\hbar$=c=1)

$$\Psi^{\pm}_{\mathrm{med}}(x) = \frac{1}{\sqrt{2\Omega_{\mathbf{k}}}}\mathrm{e}^{\mp\mathrm{i}\Omega_{\mathbf{k}}t+\mathrm{i}\mathbf{kx}} \quad \text{for} \quad t<0\,, \tag{1}$$

$$\Psi^{\pm}_{\mathrm{vac}}(x) = \frac{1}{\sqrt{2\omega_{\mathbf{k}}}}\left(c_{\mathbf{k}}\mathrm{e}^{\mp\mathrm{i}\omega_{\mathbf{k}}t+\mathrm{i}\mathbf{kx}} + s_{\mathbf{k}}\mathrm{e}^{\pm\mathrm{i}\omega_{\mathbf{k}}t+\mathrm{i}\mathbf{kx}}\right). \tag{2}$$

Here $\Omega_{\mathbf{k}}$ and $\omega_{\mathbf{k}}$ are the single-particle energies at momentum $\mathbf{k}$ in the two media. Continuity of $\Psi(x)$ and of

$\partial\Psi(i)/\partial t$ at transition time $t = 0$ determines the coefficients on the vacuum side to

$$c_{\mathbf{k}} = \tfrac{1}{2}\left(\sqrt{\tfrac{\omega_{\mathbf{k}}}{\Omega_{\mathbf{k}}}} + \sqrt{\tfrac{\Omega_{\mathbf{k}}}{\omega_{\mathbf{k}}}}\right) = \cosh[r_{\mathbf{k}}]\ , \tag{3}$$

$$s_{\mathbf{k}} = \tfrac{1}{2}\left(\sqrt{\tfrac{\omega_{\mathbf{k}}}{\Omega_{\mathbf{k}}}} - \sqrt{\tfrac{\Omega_{\mathbf{k}}}{\omega_{\mathbf{k}}}}\right) = \sinh[r_{\mathbf{k}}]\ , \tag{4}$$

$$\text{with} \quad r_{\mathbf{k}} = \tfrac{1}{2}\ln\tfrac{\omega_{\mathbf{k}}}{\Omega_{\mathbf{k}}}, \tag{5}$$

while due to the spatial homogeneity the spatial momentum $\mathbf{k}$ remains unchanged. Within the standard relativistic quantum field theory (RQFT) interpretation of the negative energy components as antiparticles with opposite spatial momenta, cf. Fig. 1 right frame, this result identically reproduces that given in Refs. [1, 4] within the BV picture. In particular the ratio of the antiparticle over particle component on the vacuum side

$$\mathcal{A} = \left|\frac{s_{\mathbf{k}}}{c_{\mathbf{k}}}\right| = \left|\frac{\Omega_{\mathbf{k}} - \omega_{\mathbf{k}}}{\Omega_{\mathbf{k}} + \omega_{\mathbf{k}}}\right| \tag{6}$$

is the analog of the well known reflection coefficient for a wave traversing from one medium to another (Fig. 1 left)

$$\mathcal{R} = \left|\frac{K - k}{K + k}\right|. \tag{7}$$

Here K and k denote the moduli of the spatial momenta in the two media. In the spatial case solely $k_\perp$ is discontinuous (ω and $\mathbf{k}_\parallel$ are continuous). In the sudden case, however, $\mathbf{k}$ is continuous, while the discontinuity in time causes a discontinuity in ω thereby creating a second component with negative ω, i.e. an antiparticle with opposite spatial momentum $\mathbf{k}$ (Fig. 1 right frame). This mechanism led to the back-to-back particle–antiparticle correlation picture advocated in Ref. [1]. Besides small antiparticle components arising form the existing particles in the medium, the time dependent interaction can also create genuine particle–antiparticle pairs out of the vacuum. The latter, which is the bosonic analog to the Dirac case, where a time-dependent interaction pulse can lift a particle from the filled Dirac sea to the particle space[1], can formally be included by adding a "+1" to the boson occupations $n_{\mathbf{k}}$ of the antiparticles. After the transition the one-body density becomes

$$n_1(\mathbf{k}) = |c_{\mathbf{k}}|^2 n_{\mathbf{k}} + |s_{\mathbf{k}}|^2(n_{\mathbf{k}} + 1) \tag{8}$$

$$n_{\mathbf{k}} = \frac{1}{\exp(|\Omega_{\mathbf{k}}|/T) + 1}, \tag{9}$$

while the back-to-back correlation function of particle–antiparticle pairs over the product of single yields becomes [4]

$$C_2(\mathbf{k}, -\mathbf{k}) = \frac{n_2(\mathbf{k}, -\mathbf{k})}{n_1(\mathbf{k}) n_1(-\mathbf{k})} \tag{10}$$

$$= 1 + \frac{|c^*_{\mathbf{k}} s_{\mathbf{k}} n_{\mathbf{k}} + c^*_{-\mathbf{k}} s_{-\mathbf{k}}(n_{-\mathbf{k}} + 1)|^2}{n_1(\mathbf{k}) n_1(-\mathbf{k})} \tag{11}$$

$$\underset{|s_{\mathbf{k}}|\ll 1}{\longrightarrow} 1 + |s_{\mathbf{k}}|^2 \left|\frac{2n_{\mathbf{k}} + 1}{n_{\mathbf{k}} + |s_{\mathbf{k}}|^2(n_{\mathbf{k}} + 1)}\right|^2, \tag{12}$$

provided the single particle yields obey the thermal distributions (9). Due to the sudden pair creation processes this back-to-back correlation ratio can attain huge values, once the statistical occupations $n_{\mathbf{k}} \sim \mathrm{e}^{-\Omega_{\mathbf{k}}/T}$ fall below $|s_{\mathbf{k}}|^2 \sim 1/\Omega^2_{\mathbf{k}}$. The subsequent considerations will show that this effect is an artifact resulting from the sudden limit.

III. THE CONTINUOUS TRANSITION CASE

Compared to the BV transformation considered in [1, 4] the wave dynamical picture used here can easily be generalized to the continuous transition case by solving the time dependent Klein-Gordon equation (suppressing in the following the dependence on spatial momentum $\mathbf{k}$)

$$\left(\partial_t^2 + \Gamma(t)\partial_t + \omega^2 - \Pi(t)\right)\Psi(t) = 0. \tag{13}$$

Here the scalar mean field[2]

$$\Pi^{\mathrm{R}}(t) = \Pi^{\mathrm{R}}(-\infty)F(t). \tag{14}$$

and $\Gamma(t)$ describe the local in-medium mass change and the damping of the particles, respectively. The latter is responsible for the continuous freeze-out [7–9] of the created pair. In the later discussion negative times refer to the situation in the medium, while the vacuum case is attained for large positive times. Thereby $F(t)$, cf. Fig. 2 below, will later be used to parameterize the transition profile. Since the here discussed observables are sensitive to time Fourier components, it is of utmost importance that the dynamical variables obey the analyticity constraints from the underlying theory. The latter provides equations of motion which from very general grounds are always given by partial differential equations in space-time. *Thus all dynamical variables and their space-time derivatives (up to infinite order) have to be continuous.* This constraint directly discards models where one switches from one analytic behavior to another one, as in the sudden limit or in case one switches from a constant behavior to an exponential decay as used in

[1] In the Dirac case also spatial transitions (Fig. 1 left) lead to spontaneous pair production, known as Klein paradox [6], once the vector potential changes by more than twice the rest mass.

[2] The picture can easily be generalized to also include vector potentials. In general the polarization functions Π can also be nonlocal in time and thus be energy dependent in the semi-classical interpretation. For the example cases discussed here we will discard such generalizations and stick to time local scalar cases.

Ref. [4]. On the other hand it allows to use methods of complex function theory. In this sense $\Pi(t)$ and $\Gamma(t)$ have to be analytic functions in t which are real for real times t.

Besides direct numerical solutions of the KG Eq. (13), there are approximate analytical methods to obtain quantitative results for the reflection coefficient. These concern the single reflection limit as well as refined semi-classical methods. In particular these methods permit to capture the final state absorption effect induced by the damping term in (13) through a time dependent escape probability [7–9]

$$\mathcal{P}(t) \;\approx\; \exp[-\textstyle\int_t^\infty dt'\;\Gamma(t')]. \tag{15}$$

It essentially suppresses the observation of the pairs created in the high density zone and therefore appropriately describes the continuous freeze-out dynamics [7, 8].

A. Single reflection approximation

A simple generalization of the sudden limit towards a continuous treatment is provided by the single reflection approximation (SR). In this scheme the continuous function $F(t)$ is approximated by a sequence of steps each providing a reflected wave component according to (6). In the continuum limit the coherent sum of these partial reflections leads to

$$\mathcal{A}^{\rm SR} \;=\; \int_{-\infty}^{\infty} dt\;\frac{\dot\Omega(t)}{2\Omega(t)}\mathcal{P}(t)\exp[-2{\rm i}\textstyle\int_0^t dt'\Omega(t')] \tag{16}$$

$$\;=\; \int_{-\infty}^{\infty} dt\;\Psi_{\rm f}^*(t)\dot\Omega(t)\Psi_{\rm i}(t) \quad \text{with} \tag{17}$$

$$\Psi_{\rm i}(t) \;=\; \Psi_{\rm f}^*(t) \approx \sqrt{\frac{\mathcal{P}(t)}{2\Omega(t)}}.\exp(-i\textstyle\int_0^t dt'\Omega(t')) \tag{18}$$

$$\Omega(t) \;=\; \sqrt{\omega^2-\Pi(t)} \tag{19}$$

and $\mathcal{P}(t)$ from (15). The appropriate phase coherence in (16) is approximately provided by describing the unreflected wave components of particles (i) and their antiparticle partners (f) in the semi-classical (WKB) limit (18).

Since $\dot\Omega\mathcal{P}(t)$ is peaked and limited to a narrow range in t, the antiparticle amplitude $\mathcal{A}$ is essentially given by the time Fourier transformed of $\dot\Omega(t)\mathcal{P}(t)$. Here we go one approximation step further and assume that $\mathcal{P}(t)$ varies smoothly across the range where $\dot\Omega(t)$ peaks[3]. Then

$$|s_{\mathbf{k}}|^2 \;\approx\; |\mathcal{A}^{\rm SR}|^2 \approx \left|\frac{\Omega-\omega}{\Omega+\omega}\right|^2 |g(2\bar\omega)|^2\,(\mathcal{P}(\bar t\,))^2 \quad \text{with (20)}$$

$$g(\omega) \;=\; \int dt\; e^{-{\rm i}\omega t} f(t), \qquad f(t) = -\frac{dF(t)}{dt}, \tag{21}$$

[3] Short freeze-out durations could enhance the high Fourier components in (19).

with abbreviations $\Omega=\Omega(-\infty)$ and $\omega=\Omega(+\infty)$. Thereby $\bar t$ has to be chosen around the maximum of $f(t)$ with $\bar\omega = \Omega(\bar t\,)$. Thus, compared to the sudden result (6) the suppression of the antiparticle amplitude is caused by two factors: the escape probability $\mathcal{P}(\bar t\,)$ taken at the peak of the pair production times the Fourier transformation of the mean-field transition profile $g(2\bar\omega)$. The latter prescription was already used in Ref. [4]. As multiple reflections at the different steps are suppressed, this approximation solely recovers terms linear in $\Delta\Omega=\Omega-\omega$.

It is educative to inspect some analytically solvable examples. As such they may not be too realistic for discussed nuclear collision dynamics, however they help clarifying the qualitative behavior of $g(\omega)$. In particular case (c), for which the KG equation is exactly solvable, provides quantitative insight into the validity regimes of the here discussed approximations.

	$F(t)$	$f(t)$	$g(\omega)$
(a)	$\frac{1}{2}-\frac{1}{\pi}\arctan\frac{\pi t}{2\tau}$	$\frac{2\tau}{\pi^2t^2+4\tau^2}$	$\mathrm{e}^{-\lvert 2\omega\tau/\pi\rvert}$
(b)	$\frac{1}{2}-\frac{1}{\pi}\arctan\big(\sinh\frac{\pi t}{2\tau}\big)$	$\frac{1}{2\tau\cosh(\pi t/(2\tau))}$	$\frac{1}{\cosh(\omega\tau)}$
(c)	$\frac{1}{\exp(2t/\tau)+1}$	$\frac{1}{2\tau\cosh^2(t/\tau)}$	$\frac{\pi\omega\tau}{2\sinh(\pi\omega\tau/2)}$

(22)

For all three cases given in Table (22) and plotted in Fig. 2, $F(t)$ monotonically falls[4] from 1 to 0 with a maximum time derivative at $t=0$ of $f(0)=-\dot F(0)=1/(2\tau)$, cf. Fig. 2. Then during the time span τ, the value of $F(t)$ will drop from 3/4 to about 1/4. These functions are similar to each other close to $t=0$ but significantly deviate in their asymptotic behavior. While for large times t case (a) falls as an inverse power law in t, case (b) and (c) drop exponential. The standard Gaussian case for $f(t)$ trivially leads to the by far steeper Gaussian suppression in ω as already discussed in Refs. [2, 3].

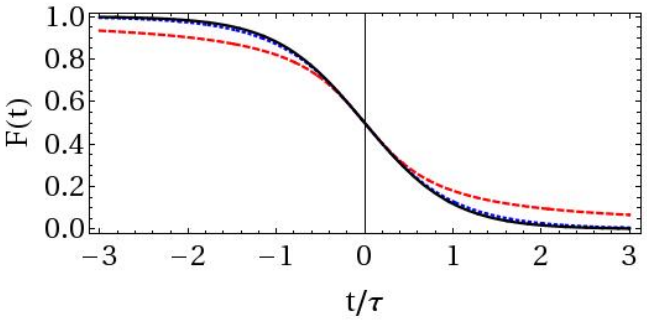

FIG. 2: (Color online) $F(t)$ for the three example cases of table (22), (a) red dashed, (b) blue dotted, (c) black full line.

[4] I exclude oscillatory behavior of $F(t)$ as it could arise e.g. from the dynamics of disoriented chiral condensates, cf. [10]. Such oscillations can augment the effect at matching frequencies.

For short transitions durations $\tau \to 0$, one verifies the sudden result (6), since then $g(2\omega) \to 1$. For large $\bar{\omega}\tau$ all three cases indeed lead to exponential suppression factors

$$|g(2\bar{\omega})|^2 \underset{\bar{\omega}\tau \gg 1}{\longrightarrow} C\ \mathrm{e}^{-4\alpha\bar{\omega}\tau} \tag{23}$$

with $C = (1, 4, (4\pi\bar{\omega}\tau)^2)$ and $\alpha = (2/\pi, 1, \pi/2)$ for the cases (a) to (c) of (22). Thereby the asymptotic exponential behavior is directly determined by the imaginary part of the nearest complex pole position of $F(t)$ through residue techniques. Similarly, branch-cut techniques can be used in the case of close complex branch points.

The cases where the polarization function is smoothly switched on and off, i.e where $F(t)$ takes the form of a bell shape, can simply be retrieved by replacing $F(t)$ by $F_{\rm bell}(t) = 2\tau f(t)$ with $f(t)$ from table (22). The corresponding "pulse" has a maximum of 1 and a time integral of 2τ. The suppression factor (23) for the pair production then will simply attain an additional pre-exponential factor of $(4\bar{\omega}\tau)^2$.

B. Complex semi-classical method (CWKB)

An alternative method to access the reflected wave component is provided by the *complex* WKB method [11]. In that case the "reflected" wave component results from the analytic continuation of the "unreflected" WKB wave $\Psi_{\rm i}$, cf. Eq. (18), around the nearest *complex valued* turning point t_0 where $\Omega^2(t_0) = \omega^2 - \Pi(t_0) = 0$. Again for simplicity and clarity the damping part will be treated perturbatively. Then the reflection coefficients $\mathcal{R}$ or $\mathcal{A}$ are given by [11]

$$\mathcal{A}^{\rm CWKB} = \mathcal{P}(\bar{t}\,)\ \exp[-2|\mathrm{Im}\ S(t_0)|], \tag{24}$$

where $\bar{t} \approx \mathrm{Re}\ t_0$ and

$$\mathrm{Im}\ S(t_0) \ = \ \mathrm{Im} \int_{t_0}^{t} dt' \sqrt{\Omega^2(t')}, \quad (\text{for real } t) \tag{25}$$

$$= \int_{t_0}^{\mathrm{Re}\ t_0} dt' \sqrt{\omega^2 - \Pi(t')} \tag{26}$$

is the mean-field action integral from the nearest complex turning point t_0 to some time t on the real axis. Since the action integral along the real axis does not contribute to Im S, one can simply choose the integration contour just parallel to the imaginary axis starting from t_0 till the real axis, cf. Eq. (26). Assuming that along this contour the integrand can essentially be approximated by its value on the real axis till close to the turning point t_0 one obtains a rough estimate

$$\mathrm{Im}\ S(t_0) \approx -\Omega(\mathrm{Re}\ t_0)\ \mathrm{Im}\ t_0\ . \tag{27}$$

For the three analytic cases of table (22) one verifies that the complex turning points are located close to the pole positions of $F(t)$ with values for $\mathrm{Im}\ t_0 = \alpha\tau$ with $\alpha = 2/\pi$, 1 and $\pi/2$, respectively for the cases (a) to (c) in (22). Thus, the pair creation rate then becomes

$$|s_{\mathbf{k}}|^2 \approx |\mathcal{A}^{\rm CWKB}|^2 \approx (\mathcal{P}(\bar{t}\,))^2\ e^{-4\alpha\bar{\omega}\tau} \tag{28}$$

in agreement with the leading exponential terms of the single reflection approximation given in (23).

The CWKB method is capable to provide some general boundary on the high ω behavior of the pair creation rate. Namely, evaluating the derivative of the action integral (26) with respect to ω one obtains

$$\left| \omega \frac{d}{d\omega}\ \mathrm{Im}\ S(t_0) \right| \geq |\mathrm{Im}\ S(t_0)|\,. \tag{29}$$

This implies that Im S can even grow faster than proportional to ω. Thus, the exponential form (28) represents an *upper bound* for the pair creation rate

$$|s_{\mathbf{k}}|^2 \approx |\mathcal{A}^{\rm CWKB}|^2 < (\mathcal{P}(\bar{t}\,))^2\ e^{-4\bar{\alpha}\bar{\omega}\tau} \tag{30}$$

with appropriately chosen $\bar{\alpha}$ of order 1. This naturally includes Gaussian and other forms that decay more steeply than exponential. For the above proof, relation (29) is rigorous if Re $\Pi(t) > 0$ along the integration path in (26), while it is expected also to hold if Re $\Pi(t)$ is negative for real t, since the main contribution to Im $dS(t_0)/d\omega$ comes from the region close to the turning point t_0, where $\Pi(t) \approx \omega^2$ is positive. The latter statement is supported by Eq. (20), which shows the pair creation rate essentially to be independent of the sign of $\Pi(t)$.

C. The exact Fermi function case

The Fermi-function case (22c) is particularly interesting, since the corresponding KG equation (13) can be solved in closed form, providing the exact result [12]

$$\mathcal{A}^2_{\rm Fermi} = \left| \frac{\sinh(\pi(\Omega - \omega)\tau/2)}{\sinh(\pi(\Omega + \omega)\tau/2)} \right|^2 \tag{31}$$

for the zero damping case $\Gamma(t) = 0$. It generalizes the sudden result (6) to the continuous Fermi-function case (22c) and further confirms the limiting cases of the single-reflection approximation (20) and the CWKB result (28) within their validity ranges. Also the corresponding action integral (26) and thus its imaginary part can be obtained in closed form

$$S_{\rm Fermi}(t_0, t) = \Omega\tau\ \mathrm{artanh}\frac{\Omega(t)}{\Omega} - \omega\tau\ \mathrm{artanh}\frac{\Omega(t)}{\omega} \tag{32}$$

$$|\mathrm{Im}\ S_{\rm Fermi}(t_0, t)| = \frac{\pi}{2}\ \mathrm{Min}(\Omega, \omega)\ \tau \quad (\text{for real } t), \tag{33}$$

the imaginary part resulting from that artanh function with argument larger than 1. The corresponding CWKB amplitude (24) then becomes

$$|\mathcal{A}^{\rm CWKB}_{\rm Fermi}|^2 \ = \exp\left[-2\pi\ \mathrm{Min}(\Omega, \omega)\ \tau\right], \tag{34}$$

in full agreement with the semi-classical limit ($\omega\tau \gg 1$, $\Delta\Omega\tau \gg 1$) of the exact Fermi-function result (31).

IV. DURATION TIME ESTIMATES

The late phase of nuclear collisions is essentially described by a thermal gas of interacting baryons and mesons that are in the process to decouple and freeze out, superimposed by a collective flow pattern dominated by radial flow. In my recent paper on continuous decoupling and freeze-out [7, 8] (see also[13]) it was shown that hadrons decouple during a time span during which the system's volume essentially grows by a factor five. This is the time window during which the here discussed particle-antiparticle pairs also can escape. For nuclear collisions with a freeze-out temperature T and a correspondingly smooth time dependence of the polarization function $\Pi(t)$ and damping rate $\Gamma(t)$, the back-to-back correlation (12) at high particle energies $\omega_{\mathbf{k}}$ can then be estimated from the upper bound (30) to

$$\begin{aligned} |c_2(\mathbf{k},-\mathbf{k})-1| &\approx |s_{\mathbf{k}}|^2/n_{\mathbf{k}}^2 \\ &\lesssim (\mathcal{P}(\bar{t}))^2\, \mathrm{e}^{-\omega_{\mathbf{k}}(4\alpha\tau-2/T)}, \end{aligned} \qquad (35)$$

valid for $|s_{\mathbf{k}}|^2 \ll n_{\mathbf{k}} \ll 1$. Here $\bar{t}$ is the time of maximum mean-field emission, while τ denotes the corresponding duration. The corresponding pairs result from creation of "off the vacuum", i.e. from the "+1" term in the Bose occupations in (12). The above estimate is rigorous and quantitative, once the semi-classical conditions are fulfilled, i.e. once $\omega\tau \gg 1$.

The effect of the mean field: If the mean-field duration scale $\tau = \tau_{\rm MF}$ would be less than $1/T$ the effect would indeed be huge. However, the characteristic times scales available to the *closed* dynamics are given by the single particle energies and thus typically of the order of T. The averaging procedure that determines the mean field Π essentially wipes out these microscopic time scales and the mean field is predominately proportional to the (baryon) density $\rho(t)$ of the system. Then the duration $\tau_{\rm MF}$ can be obtained from the collective behavior, which is mainly inertia controlled. The peak emission is then expected to occur at densities around half its average maximum value within the hadronic phase. The time during which the density drops from 3/2 of its value at peak $\rho(t_{\rm MF})$ emission to 1/2 is then given by $\tau_{\rm MF} \approx 0.5 R_{\rm MF}/v_{\rm radial}$, where $R_{\rm MF}$ is the averaged radius of the collision zone at peak emission. With typical radial flow velocities of about $v_{\rm radial} \approx 0.5$ c and $R_{\rm MF} > 5$ fm (corresponding to $\rho(t_{\rm MF})$ of less than 5 times the nuclear saturation density in central collisions) one arrives at $\tau \approx \tau_{\rm MF} > 5$ fm/c well in line with experiences from transport simulations.

Freeze-out dynamics: Let me start with some general comments about the continuous freeze-out duration and the option to determine it from experimental data. The authors of Refs. [1, 4] argued in favor of their sudden transition picture with the short freeze-out durations putatively suggested by the overall success of freeze-out models. However, none of the measured data can provide controlled estimates about the duration of the freeze-out, neither flow nor Hanbury-Brown–Twiss (HBT) investigations. Radial flow and the special HBT radius $R_{\rm long}$ may be capable to constrain the averaged freeze-out time, but not its overall duration. Due to energy conservation the transverse momentum spectra and due to a near isentropic expansion the HBT radii are very robust towards a change in the freeze-out prescription, both with respect to the absolute freeze-out time as well as its overall duration. In particular the very short freeze-out durations of 2 fm/c or less, which were claimed to be deduced from measured HBT radii at SPS and RHIC, cf. e.g. [14, 15], are absolutely meaningless [7, 8]. The reason is that the employed analysis method *completely ignores space-time correlations* which are known to develop during the expansion phase of the reaction essentially due to entropy conservation[5]. There are indeed no transport theoretical investigations that ever showed freeze-out duration anywhere as low as 2 fm/c. Indeed as recently shown in Refs. [16–19], the developing space-time correlations cause the special HBT radius $R_{\rm out}$ to be essentially insensitive to the freeze-out duration[5]. Despite the long freeze-out phase with durations up to 10 fm/c found for pions in the calculations of Refs. [16–18], the value of $R_{\rm out}$ agreed well with the experimentally observed value of $R_{\rm out} \approx R_{\rm side} \approx 6$ fm. Thus, for strongly interacting probes freeze-out durations well above 6 fm/c as manifestly found in transport simulations are not at all ruled out by experimental observations.

Rather the freeze-out and decoupling dynamics is specific for each individual particle. Weakly interacting particles can essentially escape freely. With increasing coupling to the medium estimated by $\Gamma(t) \approx \langle v_{\rm rel}\sigma_{\rm tot}\rho(t)\rangle$ the freeze-out window occurs at increasingly later times with peak brilliance at $t_{\rm freeze}$ and correspondingly longer durations $\tau_{\rm freeze}$ determined by [7, 8]

$$\dot{\Gamma}(t_{\rm freeze}) = -\Gamma^2(t_{\rm freeze}) \qquad (36)$$

$$\tau_{\rm freeze} = \mathrm{e}/\Gamma(t_{\rm freeze}) \qquad (37)$$

(consider e.g. $\Gamma = at^{-n}$, then $t_{\rm freeze} = \sqrt[n-1]{a/n} = \tau_{\rm freeze} n/\mathrm{e}$ with $\Gamma(t_{\rm freeze}) = n/t_{\rm freeze}$.). Therefore, for strongly interaction particle-antiparticle pairs such pions or K mesons one expects the peak mean-field emission well before the freeze-out window opens. Thus, one encounters the following time and duration ranges

$$t_{\rm MF} < t_{\rm freeze}, \quad \tau = \tau_{\rm MF} < \tau_{\rm freeze} \qquad (38)$$

with $\tau_{\rm MF} > 5$ fm/c at SPS energies and beyond, which are well in line with experiences from modern hybrid transport codes [16–19]. These estimates perfectly confirm the validity conditions underlying estimate (35) already for particle energies $\omega_{\mathbf{k}}$ just above the pion mass m_π.

---

[5] In this respect the results of a special exact solution of the hydrodynamic equations of motion [9, 20] are particularly informative. They showed that in this special case the HBT radii are completely insensitive to the freeze-out prescription.

V. SUMMARY AND CONCLUDING REMARKS

The option to create back-to-back particle-antiparticle pairs from a time-dependent spatially homogeneous mean field was reinvestigated by analytical methods. Thereby it is important that the time-dependence of the both, the mean field and the damping are given by analytic function in time t in order to avoid unphysical effects that lead to large time Fourier components. This excludes inverse power law behaviors for the energy spectrum of created pairs at large pair energies, as e.g. used in Ref. [4]. Rather analytic arguments are given that the spectrum is at least of exponential form with a characteristic energy scale given by the inverse transition duration τ between the in-medium situation and vacuum.

The above estimates and the experience from kinetic transport models show that both, the characteristic duration $\tau_{\rm MF}$ for the mean-field change as well as the continuous freeze-out duration $\tau_{\rm freeze}$ lie well above 4 fm/c for collision energies at the CERN SP and upwards. Already for charged pion pairs ($\pi^+\pi^-$) with $\omega_{\mathbf{k}} \approx 300$ MeV one has $\omega\tau > 6$, clarifying that the validity conditions, both for the single reflection approximation as well as for the complex WKB scheme are well fulfilled assuring them as quantitative tools. Thus, for such pion pairs the here discussed correlation signal (35) falls already well below the 10^{-7} level for the most favorable estimate at typical freeze-out temperatures of $T \approx 140$ MeV. Kaon or even ϕ meson pairs would even be much more strongly suppressed. Thus, *the pair creation process solely due to the time variation of the mean field becomes at least exponentially suppressed and experiments will have a hard time to isolate the effect.* For strongly interacting probes the final state escape probability $\mathcal{P}(t)$ will further reduced the observation of the effect if the main mean-field production essentially falls into the opaque region of the medium, where $(\mathcal{P}(t))^2 \ll 1$.

The discussed particle–antiparticle correlation effect rests on a coherent single-particle picture. Among others it largely ignores collisional effects that are known to dominate the nuclear collision dynamics. Thus, in individual events the one-body field will depart from the ensemble mean due to fluctuations caused by stochastic processes. Such microscopic processes can involve much shorter time scales which, however, are also ultra violet restricted by the frequencies accessible in the system. For thermal systems this limit is given by the inverse temperature scale, i.e. $\tau > 1/T$, limiting the "thermal" production of *hard* probes, such as the particle–antiparticle pairs. Such stochastic processes generally add incoherently to the two-particle yield. Therefore they can appropriately be included in transport codes by simulating the corresponding microscopic collision processes. The resulting pair correlations, however, are then no longer back-to-back, as they are influenced by thermal motion.

The question, whether a process can be treated in the sudden limit or not, depends on its intrinsic quantum time scale resulting from the uncertainty principle to $\tau_Q \approx 1/\Delta E$, where ΔE is the energy transfer. Driven by a certain field, the dynamics is "sudden", if the typical time duration τ, during which the field changes, is short compared to τ_Q: then the wave functions stay "inert" across the transition thereby creating several components in the eigenstates of the "new" Hamiltonian. In the opposite limit $\tau \gg \tau_Q$ the quantum states change and adjust adiabatically. As shown here for the pair creation case, where $\Delta E \approx 2\omega_{\mathbf{k}}$, the creation of states involving an energy transfer $\Delta E \gg 1/\tau$ then becomes *at least* exponentially suppressed.

Acknowledgement

The author acknowledges constructive discussions with P. Braun-Munzinger, B. Friman and D.N. Voskresensky.

[1] M. Asakawa and T. Csörgő, Heavy Ion Phys. **4**, 233 (1996).
[2] A. Vourdas and R. M. Weiner, Phys. Rev. **D38**, 2209 (1988).
[3] L. V. Razumov and R. M. Weiner, Phys. Lett. **B348**, 133 (1995).
[4] M. Asakawa, T. Csörgő, and M. Gyulassy, Phys. Rev. Lett. **83**, 4013 (1999).
[5] D. M. Dudek and S. S. Padula, Phys. Rev. **C82**, 034905 (2010).
[6] O. Klein, Z. Phys. **53**, 157 (1929).
[7] J. Knoll, Nucl. Phys. **A821**, 235 (2009).
[8] J. Knoll, Acta Phys. Polon. **B40**, 1037 (2009).
[9] Y. M. Sinyukov, S. V. Akkelin, and Y. Hama, Phys. Rev. Lett. **89**, 052301 (2002).
[10] J. Randrup, Phys. Rev. **D63**, 061901 (2001).
[11] J. Knoll and R. Schaeffer, Annals Phys. **97**, 307 (1976).
[12] S. Flügge, *Rechenmethoden der Quantentheorie* (Springer Berlin Heidelberg New York, 1965).
[13] B. Friman et al., *The CBM Physics Book, Compressed Baryonic Matter in Laboratory Experiments;* Lecture Notes in Physics, Vol. 814 (Springer Berlin Heidelberg New York, 2010), Part III, Sect. 5.8, electronic authors' version: http://www.gsi.de/forschung/fair_experiments/CBM/PhysicsBook.html.
[14] D. Adamova et al. (CERES), Nucl. Phys. **A714**, 124 (2003).
[15] S. Afanasiev et al. (PHENIX), Phys. Rev. Lett. **100**, 232301 (2008).
[16] S. V. Akkelin, Y. Hama, I. A. Karpenko, and Y. M. Sinyukov, Phys. Rev. **C78**, 034906 (2008).
[17] S. Pratt and J. Vredevoogd, Phys. Rev. C **78**, 054906 (2008), Erratum-ibid. C **79**, 069901 (2009).
[18] S. Pratt, Phys. Rev. Lett. **102**, 232301 (2009).
[19] I. A. Karpenko and Y. M. Sinyukov, Phys. Rev. **C81**, 054903 (2010).
[20] P. Csizmadia, T. Csörgő, and B. Lukacs, Phys. Lett. **B443**, 21 (1998).